Absolute Rate Constants for the Reaction $H + O_2 + M \rightarrow HO_2 + M$ over the Temperature Range 203–404 K[1a]

by Michael J. Kurylo[1b]

National Bureau of Standards, Washington, D. C. 20234 *(Received July 28, 1972)*

Publication costs assisted by Climatic Impact Assessment Program, Office of the Secretary, Department of Transportation

Absolute rate constants for the reaction $H + O_2 + M \rightarrow HO_2 + M$ have been measured by the flash photolysis–resonance fluorescence technique. For M = He, rate measurements over the temperature range 203–404 K and pressure range 10–400 Torr gave the Arrhenius expression $k_1^{He} = [6.66\ (+1.2, -1)] \times 10^{-33} \exp[(473 \pm 92)\text{cal mol}^{-1}/1.987T]\ \text{cm}^6\ \text{molecule}^{-2}\ \text{sec}^{-1}$. Comparisons of third-order rate constants at 298 K gave relative deactivation efficiencies of $CH_4/N_2/He/Ar = 15.7:3.4:1.0:1.0$. The efficiency ratio of N_2 to He was 4.5 at 226 K.

The combination reaction of atomic hydrogen with molecular oxygen is the dominant loss mechanism for H atoms in both the troposphere and stratosphere, thereby serving as a source for the hydroperoxyl (HO_2) radical. The reaction also serves as the chain termination step at the second explosion limit of the hydrogen–oxygen system. To date, kinetic studies of the $H + O_2 + M$ reaction consist of numerous high-temperature shock tube and flame data[2–5] and scattered experiments near 300 K by both direct[6–13] and indirect[14] techniques. Until recently few data were available below 300 K, and Arrhenius parameters were subject to rather large uncertainties.

To assess the role of this reaction in the chemistry of the stratosphere, accurate values of the rate parameters for various inert gases (M) over a temperature range extending to 200 K must be known. Determinations from high-temperature data (near 1000 K) are inadequate due to the errors involved in long extrapolations. Data at lower temperature have been obtained predominantly from discharge flow systems where the H-atom concentrations were followed by a calorimetric probe,[7] HNO emission,[6] mass spectroscopy,[8] and electron spin resonance spectroscopy.[10,12] These flow data are complicated by wall reactions and often require large corrections for longitudinal diffusion of H atoms and loss of H atoms by reaction with HO_2. More recent studies with static systems have employed kinetic absorption spectroscopy using pulse radiolysis[9] and mercury photosensitization[11] for atom production.

Because of the overall uncertainties in the rate constant conditions applicable to atmospheric modeling, we have undertaken a flash photolysis–resonance fluorescence study of the chemical system over a range of temperature and inert gas pressure comparable to atmospheric conditions. Experimental conditions were chosen such that stoichiometric corrections due to secondary reactions were not needed.

Experimental Section

The apparatus and technique have been described in detail previously.[15,16] In the present experiments, mixtures of an H-atom source compound (CH_4 or

(1) (a) Contribution of the National Bureau of Standards, Washington, D. C. (b) Supported in part by the Climatic Impact Assessment Program, Office of the Secretary, Department of Transportation.

(2) (a) R. R. Baldwin, L. Mayor, and P. Doran, *Trans. Faraday Soc.*, **56**, 92 (1960); (b) R. R. Baldwin and P. Doran, *ibid.*, **57**, 1578 (1961); (c) R. R. Baldwin, P. Doran, and L. Mayor, *Symp. (Int.) Combust., [Proc.] 8th*, 103 (1962); (d) R. R. Baldwin, *Symp. (Int.) Combust., [Proc.] 9th*, 218 (1963); (e) R. R. Baldwin, R. B. Moyes, B. N. Rossiter, and R. W. Walker, *Combust. Flame*, **14**, 181 (1970).

(3) (a) R. W. Getzinger and G. L. Schott, *J. Chem. Phys.*, **43**, 3237 (1965); (b) R. W. Getzinger and L. S. Blair, *Combust. Flame*, **13**, 271 (1969); (c) L. S. Blair and R. W. Getzinger, *ibid.*, **14**, 5 (1970).

(4) (a) D. Gutman, E. A. Hardwidge, F. A. Dougherty, and R. W. Lutz, *J. Chem. Phys.*, **47**, 4400 (1967); (b) G. Dixon-Lewis and A. Williams, *Symp. (Int.) Combust., [Proc.] 11th*, 951 (1967).

(5) W. G. Browne, D. R. White, and G. R. Smookler, *Symp. (Int.) Combust., [Proc.] 12th*, 557 (1968).

(6) (a) M. A. A. Clyne, *Symp. (Int.) Combust., [Proc.] 9th*, 211 (1963); (b) M. A. A. Clyne and B. A. Thrush, *Proc. Roy. Soc., Ser. A*, **275**, 559 (1963).

(7) F. S. Larkin and B. A. Thrush, *Discuss. Faraday Soc.*, **No. 37**, 112 (1964).

(8) A. F. Dodonov, G. K. Lavrovakaya, and V. L. Talrose, *Kinet. Katal.*, **10**, 701 (1969).

(9) (a) W. P. Bishop and L. M. Dorfman, *J. Chem. Phys.*, **52**, 3210 (1970); (b) T. Hikida, J. A. Eyre, and L. M. Dorfman, *ibid.*, **54**, 3422 (1971).

(10) A. A. Westenberg and N. de Haas, *J. Phys. Chem.*, **76**, 1586 (1972).

(11) J. Michael, private communication.

(12) G. K. Moortgat and E. R. Allen, presented at 163rd National Meeting of the American Chemical Society, Boston, 1972.

(13) W. Wong and D. D. Davis, private communication.

(14) Several references are cited in D. L. Baulch, D. D. Drysdale, D. G. Horne, and A. C. Lloyd, "Evaluated Kinetic Data for High Temperature Reactions," Vol. 1, Butterworth & Co., London, 1972.

(15) W. Braun and M. Lenzi, *Discuss. Faraday Soc.*, **44**, 252 (1967).

(16) (a) M. J. Kurylo, N. C. Peterson, and W. Braun, *J. Chem. Phys.*, **53**, 2776 (1970); **54**, 943 (1971); **54**, 4662 (1971); (b) D. D. Davis, R. E. Huie, J. T. Herron, M. J. Kurylo, and W. Braun, *ibid.*, **56**, 4668 (1972); (c) M. J. Kurylo, *Chem. Phys. Lett.*, **14**, 117 (1972).

C_3H_8), O_2, and an inert diluent (He, Ar, or N_2) were flash photolyzed at wavelengths above 105 nm producing on the order of 0.1 to 0.01 mTorr of atomic hydrogen. A Lyman α-resonance lamp[16a,17] operated continuously was used to excite a small fraction of the atoms, and the atom decay in the mixture was monitored by following the Lyman α-resonance fluorescence with a magnetic electron multiplier placed at right angles to both the flash and resonance lamps. Emissions from the resonance lamp at wavelengths other than 121.6 nm were filtered out by using a molecular oxygen filter between the resonance lamp and the reaction cell. In this way no interference due to resonance fluorescence from O atoms, also produced by the flash, was obtained. This was checked by flashing mixtures containing only inert gas and O_2. Fluorescence signals were accumulated on a multichannel analyzer and treated by nonlinear least-squares analysis. Since as many as 200 flashes were sometimes used to generate one kinetic curve (Figure 1), the reaction mixture was changed several times to avoid depletion of atom source or O_2 and accumulation of any reactive product species. Atom concentrations were varied by changing either the hydrocarbon pressure or the flash energy. This made it possible to assess the importance of H-atom depletion by reaction with HO_2 according to the scheme

$$H + O_2 + M \longrightarrow HO_2 + M \quad (1)$$

$$H + HO_2 \longrightarrow 2OH \quad (2)$$

Similar intensity studies coupled with variation in the H atom to O atom ratio served to analyze for the possible production of H atoms by the fast reaction

$$O + OH \longrightarrow O_2 + H \quad (3)$$

Calculations were performed to estimate the importance of OH production by

$$O + RH \longrightarrow OH + R \quad (4)$$

followed immediately by reaction 3. Such secondary H-atom generation was found to be more important when propane rather than methane was used as an H-atom source and only then at the higher O-atom concentrations ($[O_2] > 500$ mTorr). These results were verified experimentally, and consequently only experiments with CH_4 as the H-atom source and $[O_2] < 500$ mTorr were used in the final analysis. Under these conditions, calculations showed that H-atom loss by

$$H + O_3 \longrightarrow O_2 + OH \quad (5)$$

where O_3 originated from

$$O + O_2 + M \longrightarrow O_3 \cdot + M \quad (6)$$

was insignificant during the time scale of our measurements (usually several milliseconds). All experiments were consequently performed under conditions not requiring stoichiometric corrections and not controlled or complicated by O-atom chemistry.

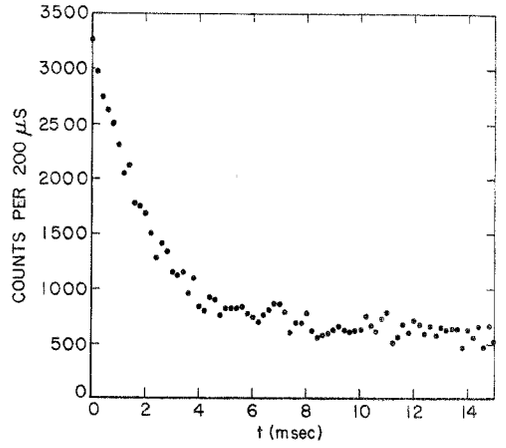

Figure 1. Typical H-atom decay curve: 200 mTorr of CH_4, 100 mTorr of O_2, 200 mTorr of He, 45-J flash energy, 298 K.

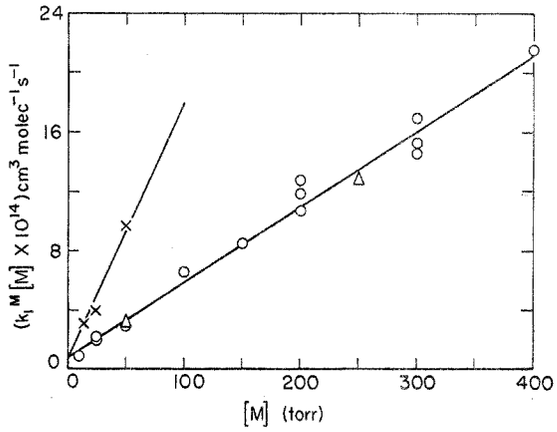

Figure 2. Plots of $k_1^M[M]$ *vs.* [M] for He (○), Ar (△), and N_2 (×) at 298 K.

Thus, in the presence of inert gas M, the loss of H atoms can be represented as

$$-\frac{d[H]}{dt} = [H][O_2]\{k_1^M[M] + k_1^{CH_4}[CH_4] + k_1^{O_2}[O_2]\} + [H]\{D + k_9[CH_4] + k_{imp}[M]\}$$

where k_1^M, $k_1^{CH_4}$, and $k_1^{O_2}$ are third-order rate constants for H–O_2 combination employing the indicated third bodies; D is the rate constant for diffusional loss of H atoms out of the viewing zone; k_9 is a bimolecular rate constant for H atom reaction with CH_4; and k_{imp} takes into account reaction with any impurity present in the inert gas. We have not included a term accounting for impurities in the oxygen since two different sources of oxygen were used without noticeable change in the atom decay rates.

(17) D. D. Davis and W. Braun, *Appl. Opt.*, 7, 2071 (1968).

Applying the foregoing analysis, the first-order H-atom decay rates at a fixed total pressure were plotted *vs.* the O_2 pressure to give slopes of $k_1^M[M] + k_1^{CH_4}[CH_4]$ and intercepts expressing the rate of H-atom loss by second-order reactions and diffusion at pressure [M]. Here we have ignored the term accounting for O_2 as a third body. Studies of the O + O_2 + M system have shown O_2 to be approximately 1.6[18] times more efficient than He or Ar. The assumption of a similar efficiency ratio in the present study would make corrections negligible. The effect of CH_4 as a third body was determined from runs in which the CH_4 concentration was varied while keeping O_2 and He fixed. By subtracting the effect of CH_4 we were thus able to obtain values for $k_1^M[M]$ the "second-order rate constant at pressure M." These second-order rate constants were then plotted against the inert gas pressure, and the slopes of these plots constitute the values of k_1^M reported here. Plots for He, Ar, and N_2 at 298 K are shown in Figure 2. This procedure was repeated at several temperatures between 200 and 400 K. The temperature study was done primarily with He as the deactivator. Although N_2 represents the most interesting M species for atmospheric applications, it serves as a very efficient quencher of Lyman α fluorescence[19] thereby greatly reducing our signal levels. Because of the difficulty in obtaining the N_2 data, values of $k_1^{N_2}$ were determined only at 298 and 226 K, the latter temperature being descriptive of the stratosphere. A value of k_1^{Ar} was determined only at 298 K.

Ultrahigh-purity gases (O_2, He, Ar, and N_2) were used without further purification. Research grade methane was degassed briefly at liquid N_2 temperature and then distilled from liquid O_2. Pressures were measured on a two-turn Bourdon gauge (20–700 Torr), a one-turn 0–20 Torr Bourdon gauge (1–20 Torr), and a capacitance manometer (<1 Torr). The calibrations of the latter two were checked frequently against a dibutyl phthalate manometer. Reaction mixtures were usually made up and stored in 2-l. glass bulbs. In experiments employing mixtures made up in the reaction cell, identical rate constants were obtained.

Results and Discussion

The experimental results of this study are presented in Tables I–IV. The precision associated with the exponential fit of the first-order decay curves was generally 3%. From these first-order rates, the second-order rate constants could be determined within an uncertainty of 5–10%. Consequently, the error associated with the final third-order rate coefficients presented in the tables is realistically assessed at 15%. Since these errors are associated with the linear fits of the data, the uncertainty could presumably be reduced by improving the statistics (*i.e.*, by increasing the number of experiments).

Table I: Rate Measurements for the Reaction H + O_2 + CH_4 → HO_2 + CH_4 at 298 K

He, Torr[a]	O_2, mTorr	CH_4, mTorr	Flash energy, J[b]	First-order rate, sec^{-1}
10	0	100	45	60.7
10	0	100	45	63.6
10	0	350	45	64.6
10	0	350	45	67.1
10	0	600	45	64.6
10	0	600	45	64.6
9.65	250	100	45	142
9.65	250	100	45	142
9.65	250	100	45	140
9.4	250	350	45	157
9.4	250	350	45	160
9.15	250	600	45	167
9.15	250	600	45	171
9.15	250	600	45	177

$k_1^{CH_4} = (24.6 \pm 7.4) \times 10^{-32}$ cm^6 $molecule^{-2}$ sec^{-1}

[a] 1 Torr = 133.32 N m^{-2} = $(9.66/T(K)) \times 10^{18}$ molecules cm^{-3}. [b] A flash energy of 80 J corresponds to an incident light intensity at the reaction cell of approximately 1×10^{13} quanta/flash.

Table II: Rate Measurements for the Reaction H + O_2 + Ar → HO_2 + Ar at 298 K

Ar, Torr[a]	O_2, mTorr	CH_4, mTorr	Flash energy, J[b]	First-order rate, sec^{-1}	$k_1^{Ar}[Ar] \times 10^{14}$, cm^3 $molecule^{-1}$ sec^{-1}[c]
50	26	200	45	109	
	50.5			125	
	100			180	
	151			243	
	200			307	
	250			333	3.14
250	25	200	45	204	
	25			189	
	50			438	
	50			410	
	100			588	
	100			647	
	150			762	
	200			943	
	225			1127	12.84

[a] 1 Torr = 133.32 N m^{-2} = $(9.66/T(K)) \times 10^{18}$ molecules cm^{-3}. [b] A flash energy of 80 J corresponds to an incident light intensity at the reaction cell of approximately 1×10^{13} quanta/flash. [c] Corrected for $k_1^{CH_4}[CH_4]$.

The rate constant for H + O_2 + CH_4 → HO_2 + CH_4 was determined at 298 K in the presence of 10 Torr of He (Table I). The value of $k_1^{CH_4}$ under the conditions

(18) F. Kaufman and J. R. Kelso, *J. Chem. Phys.*, **46**, 4541 (1967).
(19) W. Braun, C. Carlone, T. Carrington, G. Van Volkenburgh, and R. A. Young, *ibid.*, **53**, 4244 (1970).

Table III: Rate Measurements for the Reaction H + O_2 + N_2 → HO_2 + N_2

T, K	N_2, Torr[a]	O_2, mTorr	CH_4, mTorr	Flash energy, J[b]	First-order rate, sec^{-1}	$k_1^{N_2}[N_2] \times 10^{14}$, cm^3 molecule^{-1} sec^{-1} [c]	$k_1^{N_2} \times 10^{32}$, cm^6 molecule^{-2} sec^{-1}
226	5	50	300	80	70		
	5	100	300	80	131		
	5	200	300	80	213	1.80	
	30	52.5	300	80	306		
	30	105	300	80	564	11.10	8.70
298	15	15.8	180	80	112		
	15	30.6	180	80	132		
	15	61.5	180	80	172		
	15	90.6	180	80	207		
	15	120.6	180	80	213		
	15	150.6	180	80	264	3.13	
	25	26.3	300	80	131		
	25	51	300	80	174		
	25	102.5	300	80	285		
	25	151	300	80	321		
	25	201	300	80	364		
	25	251	300	80	456	3.98	
	50	25	200	80	163		
	50	50	200	80	222		
	50	102	200	80	438		
	50	150.5	200	80	569		
	50	202	200	80	722	9.80	5.33

[a] 1 Torr = 133.32 N m^{-2} = (9.66/T(K)) × 10^{18} molecules cm^{-3}. [b] A flash energy of 80 J corresponds to an incident light intensity at the reaction cell of approximately 1 × 10^{13} quanta/flash. [c] Corrected for $k_1^{CH_4}[CH_4]$.

shown was found to be 24.6 × 10^{-32} cm^6 molecule^{-2} sec^{-1} and was used to correct the Ar, He, and N_2 data as mentioned earlier. Even with 5% precision in the first-order rates, the absolute uncertainty in $k_1^{CH_4}$ is closer to 30% due to the obvious problems in measuring small differences in large numbers.

The rate constant data for H + O_2 + Ar → HO_2 + Ar at 298 K are presented in Table II. Since the values of $k_1^{Ar}[Ar]$ fell within the scatter of the similar

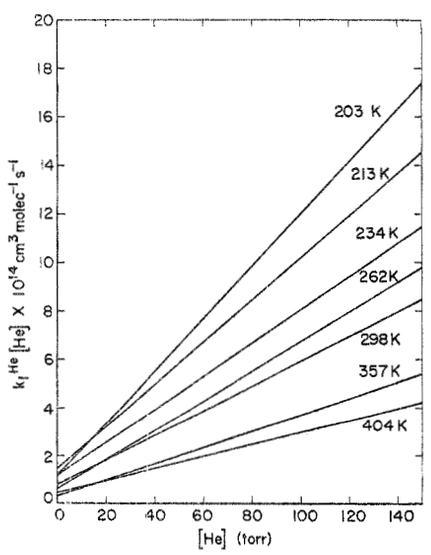

Figure 3. Plots of k_1^{He}[He] *vs.* [He] at various temperatures.

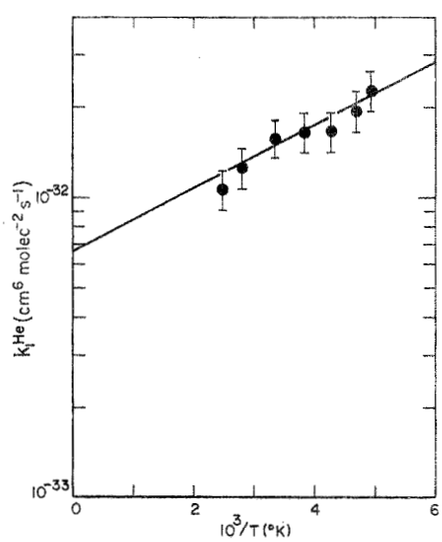

Figure 4. Arrhenius plot of the third-order rate constant for the reaction H + O_2 + He → HO_2 + He.

He data presented in Figure 2, both the Ar and He points were analyzed together to determine $k_1^{Ar,He}$. The two Ar points by themselves predict a slightly lower value for k_1^{Ar} than does the analysis used. Both approaches agree within the quoted error limits.

The data from the N_2 studies at both 298 and 226 K are shown in Table III. The analysis gives values of $k_1^{N_2}$ of 5.33 × 10^{-32} and 8.70 × 10^{-32} cm^6 molecule^{-2} sec^{-1} at 298 and 226 K, respectively.

Table IV: Rate Measurements for the Reaction H + O_2 + He → HO_2 + He

T, K	He, Torr[a]	O_2, mTorr	CH_4, mTorr	Flash energy, J[b]	First-order rate, sec^{-1}	k_1^{He}[He] × 10^{14}, cm^3 molecule^{-1} sec^{-1} [c]	k_1^{He} × 10^{32}, cm^6 molecule^{-2} sec^{-1}
203	40	24	133	55	145		
	40	48	133	55	232		
	40	80	133	55	310		
	40	120	133	55	460		
	40	160	133	55	513	5.58	
	80	48	266	55	426		
	80	96	266	55	757		
	80	160	266	55	870	9.74	
	120	72	400	55	658		
	120	144	400	55	1331		
	120	240	400	55	1688	14.24	2.27
213	30	25	127	55	126		
	30	50	127	55	185		
	30	75	127	55	240		
	30	150	127	55	332		
	30	200	127	55	494	4.04	
	60	50	253	55	246		
	60	100.7	253	55	360		
	60	200	253	55	638		
	60	300.7	253	55	931		
	60	400	253	55	1393	6.67	1.93
234	30	50	127	55	153		
	30	75	127	55	194		
	30	100	127	55	244		
	30	150	127	55	298		
	30	200	127	55	371	3.25	
	60	50	253	55	205		
	60	100.7	253	55	329		
	60	150.7	253	55	422		
	60	200	253	55	518		
	60	300.7	253	55	783		
	60	400	253	55	1018	5.30	
	100	50	253	55	270		
	100	100	253	55	438		
	100	150	253	55	615		
	100	200	253	55	842		
	100	300	253	55	1070		
	100	400	253	55	1499	8.03	1.65
262	75	25	125	55	143		
	75	50	125	55	180		
	75	75	125	55	227		
	75	100	125	55	310		
	75	150	125	55	403		
	75	200	125	55	468	5.18	
	150	50	250	55	304		
	150	100	250	55	506		
	150	200	250	55	818		
	150	300	250	55	1243	9.75	1.65
298	10	100	100	45	140[e]		
	10	200	100	45	176[e]		
	10	300	100	45	210[e]		
	10	300	100	45	188[e]		
	10	300[d]	100	45	197[e]		
	10	300	100	20	204[e]		
	10	300	100	80	202[e]		
	10	400	100	45	244[e]	0.87	
	25	10	110	45	170		
	25	25	110	45	176		
	25	50	110	45	186		
	25	100	110	45	251		
	25	150	110	45	262		
	25	200	110	45	313		

T, K	He, Torr[a]	O_2, mTorr	CH_4, mTorr	Flash energy, J[b]	First-order rate, sec^{-1}	k_1^{He}[He] × 10^{14}, cm^3 molecule^{-1} sec^{-1} [c]	k_1^{He} × 10^{32}, cm^6 molecule^{-2} sec^{-1}
298	25	300	110	45	372	2.09	
	25	0	100	45	91		
	25	0	100	45	113		
	25	25	100	45	131		
	25	25	100	45	123		
	25	50	100	45	139		
	25	50	100	45	139		
	25	100	100	45	192		
	25	100	100	45	188		
	25	200	100	45	245		
	25	200	100	45	251		
	25	300	100	45	308		
	25	300	100	45	304		
	25	400	100	45	402	2.05	
	50	25	220	72	215		
	50	50	220	72	271		
	50	100	220	72	294		
	50	130	220	72	379		
	50	200	220	72	398		
	50	300	220	72	517	3.04	
	100	25	105	72	210		
	100	50	105	72	271		
	100	100	105	72	357		
	100	150	105	72	482		
	100	200	105	72	556		
	100	250	105	72	717	6.58	
	150	50	100	45	214		
	150	50	100	45	225		
	150	100	100	45	359		
	150	150	100	45	510		
	150	150	100	45	473		
	150	200	100	45	649		
	150	300	100	45	819		
	150	400	100	45	1215	8.55	
	200	50	160	45	430		
	200	50	160	45	437		
	200	100	160	45	675		
	200	150	160	45	833		
	200	200	160	45	1020	11.91	
	200	100	105	72	590		
	200	200	105	72	966		
	200	300	105	72	1429		
	200	400	105	72	1826	12.78	
	200	0	200	45	102		
	200	0	200	45	77		
	200	100	200	45	458		
	200	100	200	45	408		
	200	100	200	45	490		
	200	200	200	45	792		
	200	200	200	45	839		
	200	300	200	45	1143		
	200	300	200	45	1131	10.67	
	300	100	40	45	651		
	300	100	40	45	705		
	300	200	40	45	1097		
	300	300	40	45	1585		
	300	400	40	45	2200	15.32	
	300	37.5	150	45	281		
	300	75	150	45	468		
	300	75	150	45	495		
	300	112.5	150	45	811		
	300	150	150	45	939		
	300	150	150	45	951		

Table IV (*Continued*)

T, K	He, Torr[a]	O_2, mTorr	CH_4, mTorr	Flash energy, J[b]	First-order rate, sec^{-1}	$k_1^{He}[He] \times 10^{14}$, cm^3 molecule^{-1} sec^{-1} [c]	$k_1^{He} \times 10^{32}$, cm^6 molecule^{-2} sec^{-1}
298	300	225	150	45	1283		
	300	225	150	72	1246		
	300	225	150	187	1264		
	300	300	150	45	1499	14.61	
	300	50	240	45	738		
	300	100	240	45	997		
	300	200	240	45	1572	17.04	
	400	25	200	45	270		
	400	50	200	45	496		
	400	50	200	45	467		
	400	75	200	45	695		
	400	100	200	45	794		
	400	100	200	45	806		
	400	150	200	45	1144		
	400	200	200	45	1545	21.55	1.57
357	35	28.3	140	55	169		
	35	56.8	140	55	178		
	35	84.0	140	55	206		
	35	112.6	140	55	217		
	35	168.3	140	55	227	1.54	
	75	60.6	300	55	193		
	75	60.6	300	55	165		
	75	121.8	300	55	225		
	75	180	300	55	279		
	75	241.2	300	55	329		
	75	360	300	55	420	2.84	
	150	121.2	600	55	308		
	150	243.6	600	55	489		
	150	360.0	600	55	727		
	150	482.4	600	55	796		
	150	721.2	600	55	1258	5.41	1.25
434	50	30	167	55	211		
	50	60	167	55	232		
	50	100	167	55	234		
	50	200	167	55	295		
	50	300	167	55	327	1.75	
	150	90	500	55	219		
	150	180	500	55	317		
	150	300	500	55	444		
	150	450	500	55	595		
	150	600	500	55	772	4.28	1.06

[a] 1 Torr = 133.32 N m^{-2} = (9.66/T(K)) × 10^{18} molecules cm^{-3}. [b] A flash energy of 80 J corresponds to an incident light intensity at the reaction cell of approximately 1 × 10^{13} quanta/flash. [c] Corrected for $k_1^{CH_4}[CH_4]$. [d] Ultrahigh-purity O_2 from a Pyrex storage bulb. [e] Corrected for third-body effect of O_2 assuming $k_1^{O_2} = 1.6k_1^{He}$.

As mentioned earlier, the most extensive data were taken on the H + O_2 + He system (Table IV). These data were analyzed as for other M species with the exception that the 10-Torr He data were corrected for the third-body effect of O_2. We have taken the efficiencies of O_2 and He as deactivators to be in the same ratio as measured for the O + O_2 + M reaction.[18] The positive intercepts appearing in plots of $k_1^M[M]$ *vs.* [M] (Figure 2) are not predicted by the data analysis outlined earlier. Such intercepts could be attributed to either a radiative combination not requiring a third body or a wall component of the measured reaction. The room temperature intercept of 8 × 10^{-15} cm^3 molecule^{-1} sec^{-1} is some two orders of magnitude higher than expected for radiative combination, and we thus prefer the latter explanation. Although our observation zone is defined by the intersection of three columnated beams (flash lamp, resonance lamp, and photomultiplier) in the center of the cell, the cell used in these experiments was very small and a small fraction of the H atoms could have been observed at the walls. This explanation is consistent with the observation in Figure 3 that the intercept tends to become more positive with decreasing temperature. Measurements were therefore taken over extended pressure ranges thereby minimizing the significance of the intercept. The slope of

Table V: A Summary of Rate Data on the Reaction H + O_2 + M → HO_2 + M

T, K	M	k, cm^6 molecule^{-2} sec^{-2}	Method	Reference
298	CH_4	24.6×10^{-32}	Flash photolysis–resonance fluorescence	This work
298	Ar	1.57×10^{-32}		
298	He	1.57×10^{-32}		
203–404	He	$6.66 \times 10^{-33} \times \exp(473 \text{ cal mol}^{-1}/1.987T)$		
298	N_2	5.33×10^{-32}		
226	N_2	8.70×10^{-32}		
298	Ar	1.6×10^{-32}	Pulsed absorption spectrophotometry	Dorfman, *et al.*
298	H_2	4.7×10^{-32}		
297	Ar	1.54×10^{-32}	Discharge flow (esr)	Moortgat and Allen
297	He	1.49×10^{-32}		
297	H_2	6.34×10^{-32}		
298	Ar	1.87×10^{-32}	Discharge flow (esr)	Westenberg and de Haas
298	He	1.87×10^{-32}		
298	Ar	0.61×10^{-32}	Pulsed absorption spectrophotometry (mercury photosensitized)	Michael
298	He	3.75×10^{-32}		
298	H_2	1.22×10^{-32}		
298	Ne	3.16×10^{-32}		
298	Kr	1.1×10^{-32}		
298	Ar	1.95×10^{-32}	Flash photolysis–resonance fluorescence	Wong and Davis
298	He	1.88×10^{-32}		
298	N_2	5.3×10^{-32}		
298	CH_4	41.5×10^{-32}		
220–360	Ar	$6.75 \times 10^{-33} \times \exp(685 \text{ cal mol}^{-1}/1.987T)$		
220	N_2	8.35×10^{-32}		
293	Ar	3.3×10^{-32}	Discharge flow (HNO emission)	Clyne
293	Ar	2.2×10^{-32}	Discharge flow (HNO emission)	Clyne and Thrush
244	Ar	4.0×10^{-32}		
225	Ar	3.5×10^{-32}		
293	He	2.1×10^{-32}		
293	H_2O	52.1×10^{-32}		
293	Ar	3.7×10^{-32}	Discharge flow calorimetric probe	Larkin and Thrush
293	He	6×10^{-32}	Mass spectrometric probe of diffusional cloud	Dodonov, *et al.*

the helium and argon plot in Figure 2 gives a value for $k_1^{He} = k_1^{Ar} = 1.57 \times 10^{-32}$ cm^6 molecule^{-2} sec^{-1}. The slopes from similar plots at other temperatures (Figure 3) are presented in Arrhenius fashion in Figure 4. The Arrhenius expression, determined from a weighted least-squares treatment of the data, was found to be

$$k_1^{He} = [6.66\ (+1.2, -1)] \times 10^{-33} \exp\left[\frac{(473 \pm 92) \text{ cal mol}^{-1}}{1.987T}\right]$$

in units of cm^6 molecule^{-2} sec^{-1}. The weights for the points were chosen according to the quantity and quality of the data. The error limits given are standard deviations from the least-squares fit. An unweighted least-squares analysis of the Arrhenius data gives

$$k_1^{He} = [5.89\ (+0.80, -0.70)] \times 10^{-33} \exp\left[\frac{(522 \pm 66) \text{ cal mol}^{-1}}{1.987T}\right]$$

By making use of the full 15% error bars shown in Figure 4, the preexponential factor ranges from 4.2 to 7.6×10^{-33} cm^6 molecule^{-2} sec^{-1} and the exponential term from 380 to 700 cal/mol.

At 298 K the ratios of third-body efficiencies for stabilizing the HO_2 adduct are $CH_4/N_2/He/Ar$ = 15.7:3.4:1.0:1.0. The ratio of efficiencies of N_2 to He is 4.5:1 at 226 K. These trends in efficiencies are in good agreement with those recently observed for the O + O_2 + M reaction system.[20]

In Table V the results of the present work are summarized along with recent measurements of other workers. Excluded from the table are the numerous high-temperature flame and shock tube data as well as any other studies dealing with inert gases and temperatures outside the scope of the present work. At 298 K excellent agreement is obtained with Dorfman, *et al.*,[9] Moortgat and Allen,[12] Westenberg and deHaas,[10] and

(20) R. E. Huie, J. T. Herron, and D. D. Davis, *J. Phys. Chem.*, 76, 2653 (1972).

Wong and Davis[13] for M = He, Ar, and N_2. The difference between the $k_1^{CH_4}$ values of this work and that of Wong and Davis is within the expanded error limits which must be assigned to both values (as described earlier). The Arrhenius parameters show somewhat different temperature dependences with nearly equal A factors although both are within the quoted uncertainties. Since identical techniques were used, however, it would have been more gratifying were there better overlap in the temperature dependence. This difference in temperature dependence for He or Ar coupled with the identical N_2 results solely accounts for the discrepancy in the relative deactivation efficiency ratios at low temperature. The data of Michael[11] give rate constants much lower than those of most present studies. Whereas no definite explanation for the low values can be given at this time, it is possible that production of H atoms in the mercury hydride system could account for slower measured decay rates. We cannot say whether this would affect the measured relative deactivation efficiencies.

The uncertainties in the flow data of Clyne,[6a] Clyne and Thrush,[6b] and Larkin and Thrush[7] can be ascertained from the variation in rate constants between successive studies and temperatures. These studies required corrections for longitudinal diffusion, reaction with product species, wall reactions, and efficiencies of other inert gases present. They are not as precise or accurate as the more recent flow studies of Moortgat and Allen or Westenberg and de Haas, who were able to use information from the earlier studies in making these corrections. Nevertheless, the agreement with our present work is probably within the error limits of these earlier studies.

The high value for k_1^{He} obtained by Dodonov, *et al.*,[8] was determined by mass spectrometric probing in a diffusional cloud. The extreme uncertainties in defining the chemistry and physical boundary of the reacting system tend to question the reliability of the results.

Since our temperature coverage did not exceed 404 K, any comparisons with the previous high-temperature flame and shock tube work must rely on the validity of extrapolating our Arrhenius fit outside of our measurement range. If we assume no gross disparity from the fit in going to high temperatures, the present study predicts a change in rate constant from 7.6×10^{-33} to 8.4×10^{-33} cm^6 molecule^{-2} sec^{-1} over the temperature interval 1600–1000 K. This is to be compared with measured values of 8.3×10^{-33} (1435–1650 K),[3c] 9.1×10^{-33} (1100 K),[4a] and 3.9×10^{-33} (1500 K).[3a] Many of the similar high-temperature studies suffer from the inability to specify the M species and the necessary assignment of a complicated mechanism. All have reported uncertainties neighboring 50%.

Several reviews[14] have appeared dealing with reaction 1. The recommended Arrhenius parameters are, as explained earlier, subject to large uncertainties due to the large scatter in the high-temperature data and the lower precision and accuracy of the earlier low-temperature work. The recent review of Baulch, *et al.*,[14] assigns (in units of cm^6 molecule^{-2} sec^{-1})

$$k_1^{Ar,He} = [4.1 \pm 1.0] \times 10^{-33} \exp\left[\frac{(1000 \pm 500) \text{ cal mol}^{-1}}{1.987T}\right]$$

The present work has established the rate constant for the combination reaction of atomic hydrogen with molecular oxygen as a function of temperature for a number of collision partners. Measurements were made in a static system free from the possible large uncertainties due to secondary and wall reactions. Conditions were chosen to match those needed for atmospheric modeling. The results indicate a smaller temperature dependence of k_1^M than previously assumed as well as lower absolute values than reported in the early discharge flow work. The very recent measurements of other workers fully support these observations.

Acknowledgment. The author would like to thank the numerous workers[10-13] who made their results available prior to publication.